Formation of Hybrid Electronic States in FePc Chains Mediated by the Au(110) Surface

ARTICLE *in* THE JOURNAL OF PHYSICAL CHEMISTRY C · APRIL 2012

Impact Factor: 4.77 · DOI: 10.1021/jp300663t

THE JOURNAL OF PHYSICAL CHEMISTRY C

Article

pubs.acs.org/JPCC

Formation of Hybrid Electronic States in FePc Chains Mediated by the Au(110) Surface

Maria Grazia Betti,*[,†] Pierluigi Gargiani,[‡] Carlo Mariani,[†] Stefano Turchini,[§] Nicola Zema,[§] Sara Fortuna,[∥,⊥] Arrigo Calzolari,[¶] and Stefano Fabris[∥,⊥]

[†]Dipartimento di Fisica, CNISM, CNIS, Università di Roma La Sapienza, Piazzale Aldo Moro 2, I- 00185 Roma, Italy

[‡]Dipartimento di Fisica, Università di Roma La Sapienza, Piazzale Aldo Moro 2, I - 00185 Roma, Italy

[§]ISM-CNR, Via delFosso del Cavaliere 100, 00133 Roma, Italy

[∥]CNR-IOM DEMOCRITOS, Theory@Elettra group, S.S. 14, km 163.5, I-34149 Trieste, Italy

[⊥]SISSA, Via Bonomea 265, I-34136, Trieste, Italy

[¶]CNR-Nano Istituto di Nanoscienze, Centro S3, I-41125 Modena, Italy

Supporting Information

ABSTRACT: Iron−phthalocyanine (FePc) molecules deposited on the Au(110) surface self-organize in ordered chains driven by the reconstructed Au channels. The interaction process induces a rehybridization of the electronic states localized on the central metal atom, breaking the 4-fold symmetry of the molecular orbitals of the FePc molecules. The molecular adsorption is controlled by a symmetry-determined mixing between the electronic states of the Fe metal center and of the Au substrate, as deduced by photoemission and absorption spectroscopy exploiting light polarization. DFT calculations rationalize this mixing of the Fe and Au states on the basis of symmetry arguments. The calculated electronic structure reproduces the main experimental spectral features, which are associated to a distorted molecular structure displaying a trigonal bipyramidal geometry of the ligands around the metal center.

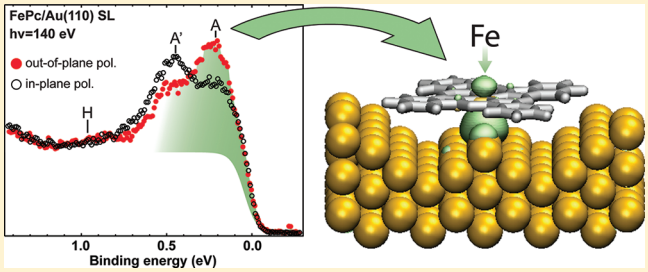

INTRODUCTION

The design of 1D and 2D architectures based on the self-assembly of metallorganic molecules is nowadays a widely exploited path, with the final objective of tailoring their electronic, transport, and magnetic properties.[1−3] The electronic, magnetic, and transport properties of simple metallorganic systems can be tuned by modifying the molecule−molecule interaction and the molecule−substrate coupling.[2,4−8] This goal requires a detailed knowledge of the evolution of the molecular orbitals when deposited on a suitable substrate and of the interaction strength at the interface. In this framework, metal−phthalocyanines ($M-C_{32}H_{16}N_8$, MPcs) represent an interesting class of metallorganic systems, as they can coordinate most of the metals of the periodic table. MPcs are stable aromatic dyes composed by four pyrrolic and four benzene rings arranged around the central metal atom, with a 4-fold symmetry as isolated molecules. They may constitute exemplary molecular biomimetic prototypes[9] for studying electronic states in different conditions of solid aggregation, by self-assembling them on templating surfaces able to drive well ordered 1D and 2D architectures.[10−12] Their charge transport and delocalization are mainly due to the π-conjugation,[13] whereas the central metal atom can be exploited to control their magnetic properties. The interaction process can reduce the 4-fold symmetry of the planar molecule as observed in similar molecular 1D and 2D structures adsorbed on metal surfaces,[14−20] affecting the electronic level ordering and symmetry, hence producing peculiar new magnetic and transport properties.

In this article, we study FePc molecular chains arranged along the Au(110) reconstructed nanorails, addressing the orbital symmetry and the electronic mixing between the organic molecular orbitals and the substrate states, by means of both experimental and theoretical approaches. FePc and CoPc deposited on Au(110) present considerable interaction of the central metal atom with the metal substrate while the benzene and pyrrole macrocycles are less involved in the process.[21,22] The purpose herewith is to follow the interaction process at the ordered FePc single-layer on Au(110), identifying the electronic states involved in the interaction, their localization, mixing, and symmetry. The electronic spectral density of states is measured by means of synchrotron-based photoelectron and absorption spectroscopy. The electronic structure and the density of states (DOS) are computed from first-principles in the framework of DFT for a model system that correctly predicts recent structural results.[23] The experimental and

Received: January 19, 2012
Revised: March 22, 2012
Published: March 26, 2012

theoretical studies provide a unified picture of molecular orbitals symmetry reduction with respect to the free molecule driven by the interaction process with the Au metallic states.

METHODS

Experimental Details. Valence-band experiments were carried out at the Circular Polarization 4.2 (POLAR) beamline and near-edge X-ray absorption fine structure (NEXAFS) data across the Fe-L_3 edge were taken at the ALOISA beamline at ELETTRA (Trieste, Italy). Valence-band data have been taken in the photon energy range 40−140 eV by means of an hemispherical electron analyzer, with 10 eV of pass-energy, corresponding to an overall energy resolution of 50 meV. Incident photons were provided by a grazing incidence monochramator for the energy range 40−170 eV.

The polarization dependent photoemission experiment was performed keeping a constant grazing incidence of impinging radiation at 20° and rotating the polarization direction from vertical to horizontal. Hence, in-plane corresponds to the electric field oriented parallel to the surface plane while out-of-plane to a 70° of incidence of the electric field. The angle between sample surface normal and electron analyzer axis was kept fixed during polarization dependent measurements. Data were collected at a sample temperature of 80 K.

The NEXAFS spectra were obtained in the partial electron yield mode by means of a channeltron facing the sample. The linear polarization in the NEXAFS data was changed by rotating the surface around the X-ray axis, while keeping a constant grazing incidence of 6°, thus obtaining the electric field oriented either in the surface plane or almost normal to it. Data have been taken with the sample kept at 150 K to minimize the radiation damage.

The clean Au(110) surface and the ordered FePc layers were prepared in ultrahigh vacuum (UHV) chambers, with base pressure of at least 5×10^{-10} mbar. Surface quality and cleanness were checked for both experiments by means of XPS. The Au(110)-(1 × 2) substrate surface was prepared by subsequent Ar^+ ion sputtering-annealing cycles at 1 keV and 720 K, followed by 500 eV and 520 K. FePc was evaporated from resistively heated boron-nitride and quartz crucibles in UHV, and the nominal thickness was measured via oscillating quartz microbalances. The FePc molecules have been deposited on the clean Au(110) substrate with a deposition rate of about 0.5 Å/min. The long-range ordered single-layer (SL) has been obtained by depositing FePc onto the gold surface kept at 430 K.[21]

Computational Details. The electronic structure of the FePc molecules adsorbed on the Au(110) surface was studied by DFT calculations with the Perdew-Burke-Ernzerhof generalized gradient corrected approximation (PBE-GGA) for the exchange and correlation energy functional.[24] The spin-polarized Kohn−Sham equations were solved in the plane-waves pseudopotential framework, as implemented in the PW scf code of the Quantum ESPRESSO distribution.[25,26] The valence wave function and charge density representation were described by a plane-wave basis set limited by 30 and 300 Ry, respectively.

The system was described with periodic supercells with lateral extension corresponding to a 5 × 5 Au(110) surface. The latter was modeled with a slab consisting of five atomic layers, separated in the z direction by more than 14 Å of vacuum, with the lattice parameter set to the calculated equilibrium value (4.18 Å). Among the possible reconstructions compatible with this periodicity, we have performed the simulations on the lowest energy FePc/Au(110) interface with 5-fold periodicity along [001] (Figure S1 of the Supporting Information).[23] During the structural relaxations the lowermost two layers were kept fixed at their bulklike coordinates. Integrals in the Brillouin zone were performed on a regular (4 × 4 × 1) **k**-point mesh together with a Marzari-Vanderbilt smearing of 0.02 Ry.

RESULTS

Photoemission, Absorption and Interaction States Symmetry. Representative photoemission spectra in the valence band energy region of a FePc single-layer deposited on the Au(110)-(1 × 2) reconstructed surface, as a function of the photon energy, are reported in Figure 1. The FePc single-layer induces the suppression of the Au(110) surface states, whereas new states due to molecule−metal interaction arise, different from the bare FePc molecular states.[21,22,27] All of these states are clearly localized at the interface, as their sharpness and intensity are maximum when the single-layer of MPc is completed.[21,22,28,29]

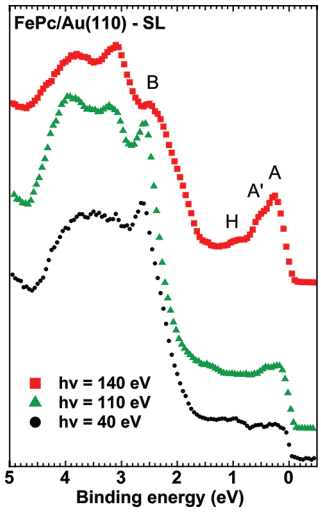

Figure 1. Normal-emission photoemission spectra of the valence band near the Fermi level for a single-layer of FePc grown on Au(110), as a function of the photon energy (40 eV, black circles; 110 eV, green triangles; 140 eV, red squares).

The electronic spectral density of states at normal emission in the low binding energy (BE) region is characterized by two main FePc-induced structures at 0.21 eV (A) and 0.45 eV (A′) respectively, and both peaks are more intense at increasing photon energies (110 and 140 eV), when the photoionization cross section favors electronic states localized on the central metal atom. A broad structure (H) occurs at 0.95 eV BE, present for all exciting photon energies, attributed to an interface macrocycle-associated state, that fully develops in the π molecular orbital with a_{1u} symmetry located on the pyrrole ring when a thick molecular film is formed.[21] In the binding energy region dominated by the Au d bands, a FePc induced state resonant with the Au d states can be clearly identified at about 2.65 eV BE (for $h\nu = 40$ eV), more intense at low photon energy, when the photoionization cross section is higher for the electronic states located on the macrocycles.

The symmetry of the FePc induced interaction states can be identified by exploiting the polarization dependent selection

dx.doi.org/10.1021/jp300663t | J. Phys. Chem. C 2012, 116, 8657−8663

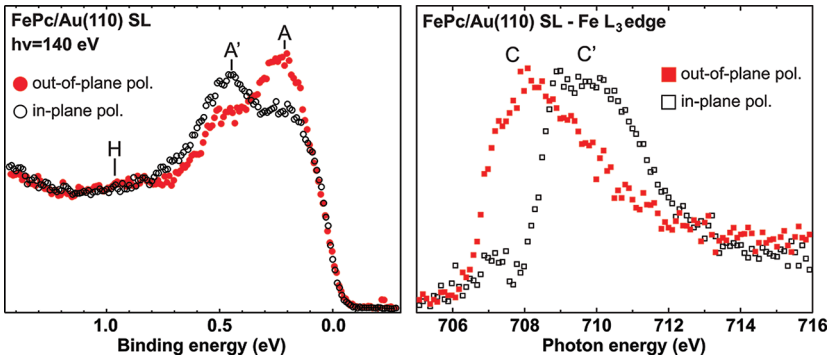

Figure 2. Left panel: Photoemission spectra of the valence band close to the Fermi level for a single-layer of FePc grown on Au(110), excited with linearly polarized radiation (in-plane, black open circles; out-of-plane, red filled circles). Right panel: Fe L_3 -edge NEXAFS data for the SL-FePc/Au(110) interface, excited with linearly polarized radiation (in-plane, black open squares; out-of-plane, red filled squares).

rules of photoemission and absorption spectroscopies. Linearly polarized radiation impinges on the surface with the electric field oriented either along the surface plane (in-plane) or out-of-plane (70° and 84° of incidence for the photoemission and absorption experiments, respectively). Both the occupied states observed by valence band photoemission and the empty levels assessed by the Fe-L_3 absorption spectra present a distinct dichroic response, as reported in Figure 2. Concerning the occupied states, the interface state A (localized at 0.21 eV BE) presents an out-of-plane orientation, whereas A′ (at 0.45 eV BE) is prevalently due to in-plane states (Figure 2, left panel). The final states with d-symmetry assessed in the NEXAFS data present two main absorption structures, C and C′, whose centroid lies at 708.2 and 709.5 eV photon energy, respectively (Figure 2, right panel). Looking at their polarization dependence, the first absorption peak C corresponds to transitions to out-of-plane states, whereas the higher energy structure C′ is associated to in-plane final states. The line shape of the Fe-L_3 edge for a single-layer of FePc on Au(110) does not present a one-to-one correspondence with the FePc thin films absorption structures[22,30] indicating an orbital mixing of the molecular orbitals located on the central metal atoms with the underlying Au metal states.

Theoretical Analysis. The symmetry and the hybridization of the electronic states for the FePc ordered chains on Au(110) can be identified by comparing the dichroic response of the photoemission and absorption data with theoretical predictions on the electronic density of states. To assign specific orbital symmetries to the structures measured by valence-band photoemission and NEXAFS, we briefly remind the reduced symmetry of the Fe 3d orbitals in a D_{4h} ligand field, resulting in three d_{z^2}, $d_{x^2-y^2}$, and d_{xy} singlet states with symmetry a_{1g}, b_{1g}, and b_{2g} respectively and in one (d_{xz}, d_{yz}) doublet state with e_g symmetry (Figure 3). The contribution of these Fe d states to the FePc molecular orbitals (MO) is determined by symmetry:

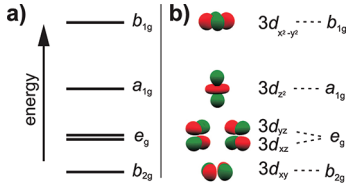

Figure 3. Sketch of the Fe-d orbitals energy in the D_{4h} point group of an isolated FePc molecule (a) and corresponding spatial distribution (b).

the e_g MO results from the interaction between the Fe (d_{xz}, d_{yz}) and the N-p_z states of the delocalized π system; the a_{1g} MO from the Fe d_{z^2} states and the N s and N $p_{x,y}$ states pointing toward the metal center; the b_{2g} MO from the Fe d_{xy} states and the N $p_{x,y}$ states orthogonal to the metal center; the b_{1g} MO from the Fe $d_{x^2-y^2}$ states and the N $p_{x,y}$ states pointing toward the metal center. The overlap between the metal and organic states determines the relative energy ordering of these MOs. A qualitative text-book scheme is displayed in Figure 3. Note however that this analysis neglects the spin dependence of the MO energies, which turns out to be quite important for magnetic metal centers, such as the present case of Fe.

The energy levels of the FePc molecule resulting from our DFT calculations with the GGA-PBE functional are displayed in panel a of Figure 4 for an energy window centered at the frontier orbitals. The molecule is predicted to be in a triplet state, with the two unpaired electrons in the single occupied molecular orbitals a_{1g} and e_g, respectively. Blue/red lines denote the organic/metallic contributions to each MO, which are labeled according to their symmetry and whose electron density is reported in panels b–i of Figure 4. The spin-polarized calculations show that the energy ordering of the metallorganic FePc states is different from the qualitative spin-independent symmetry-based analysis described above. All the MOs in panel a of Figure 4 have metallorganic character, except a_{1u}, whose wave function is fully localized on the macrocycles parts (panel e of Figure 4).

The two spin-up e_g states are occupied while the two corresponding spin-down MOs are one filled and one empty, the filled one being the HOMO-1 (panel f of Figure 4). The HOMO corresponds to the b_{2g} MO. The unoccupied unpaired e_g and a_{1g} MOs are the LUMO (panel h of Figure 4) and LUMO+1 (panel i of Figure 4) respectively, whereas the unoccupied b_{1g} MO is predicted to have much higher energies (1.9 and 3.2 eV for the up and down spins, respectively), in agreement with the ligand field theory. Note that the actual energy ordering of the free-standing FePc molecular orbitals predicted by theoretical simulations shows some variations on the exchange and correlation functional, the main issue concerning the location of the organic state a_{1u} with respect to the metallorganic states.

This ^3E_g ground state is in agreement with experimental data[30−33] and recent DFT-GGA simulations.[34] Note that other simulations predicted a $^3B_{2g}$ ground state,[35] which our calculations predict to be 0.12 eV higher in energy than the ^3E_g configuration.

dx.doi.org/10.1021/jp300663t | J. Phys. Chem. C 2012, 116, 8657−8663

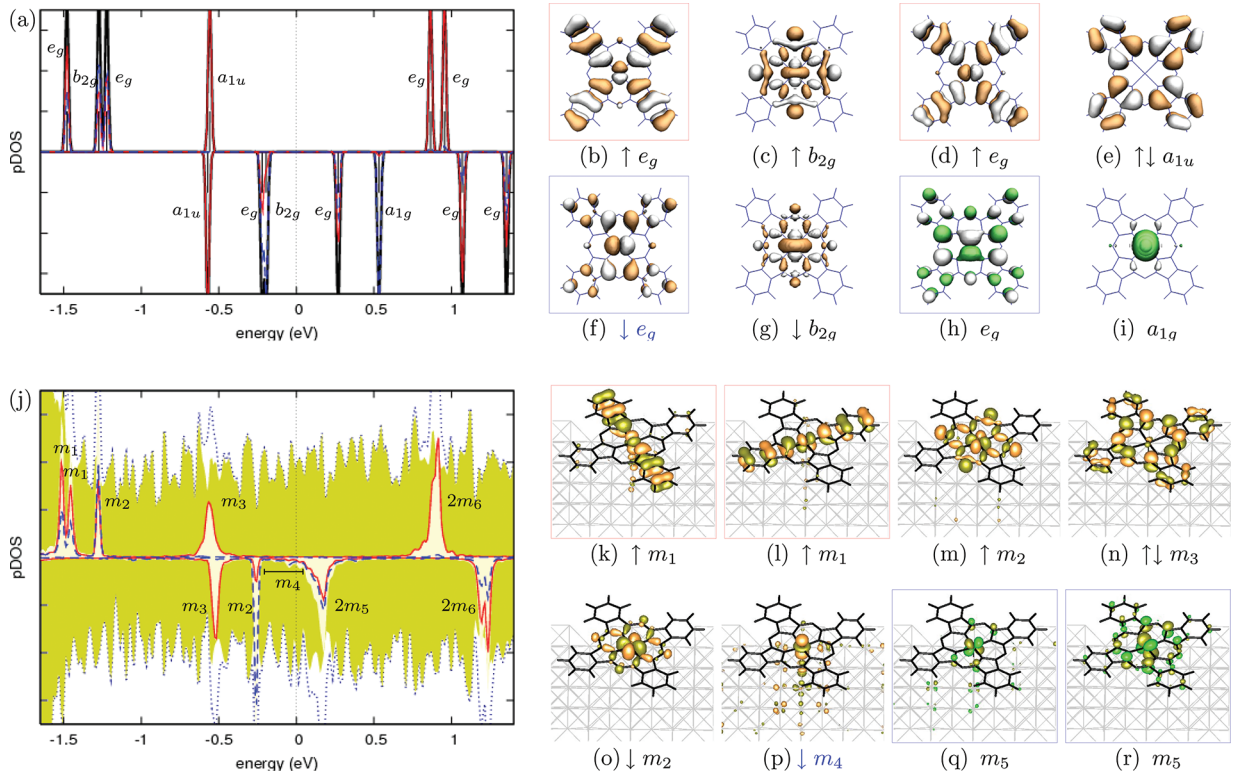

Figure 4. Upper part: (a) computed total density of states for the isolated FePc molecule (black line) and projected density of states for the Pc (red solid line) and Fe (blue dashed line), and corresponding electronic states (b–i). Lower part: (j) computed total density of states for the FePc/Au system (blue dotted line) and projected density of states for the Au (filled gold area), FePc (filled clear area), Pc (red solid line) and Fe (blue dashed line), and corresponding electronic states (k–r). Occupied/empty states are color-coded in red/green and are calculated at $\bar{\Gamma}$. Orbitals that change their relative position upon absorption are enclosed by boxes.

Our experimental results suggest that adsorption of FePc on the Au(110) surface induces electron mixing with the underlying metal states that alters the symmetry and energy ordering of the FePc molecular orbitals with respect to the free-standing ones. This is confirmed by the electronic density of states (DOS) calculated for the FePc molecule interacting with the Au(110) surface, reported in panel j of Figure 4. The electronic structure is calculated for the most stable adsorption configuration of the FePc molecule on Au(110), which comprises a complex reconstruction of the underlying surface.[23] The sequence and symmetry of the molecular states described in the present work are however not affected by the surface reconstruction. The electronic structure of the FePc molecule adsorbed on the Au surface presents some states that preserve their molecular nature and that can be directly correlated to those of the isolated molecule. In particular, the spin-up m_1 and m_2 states are the correspondent of the e_g and b_{2g} MOs in the free FePc, as evident by comparing their electron densities (panels l and d, and m and c of Figure 4). With respect to these metallorganic MOs, the energy of the organic a_{1u} states are marginally affected by the interaction with the surface and can be clearly associated to the states m_3 (panels n and e of Figure 4). The frontier states are instead much more influenced by the molecular adsorption. The sharp occupied spin-down m_2 state (panel o of Figure 4), the HOMO in the adsorbed case, resembles the spin-down b_{2g} HOMO of the unsupported FePc (panel g of Figure 4). Correspondingly, the unoccupied spin-down m_5 states (panels q and r of Figure 4) resemble the e_g states of the unsupported FePc (panels f and h of Figure 4).

The strongest effect of molecular adsorption occurs on the spin-down a_{1g} MO, which in the unsupported FePc is unoccupied and dominated by the Fe d_{z^2} orbital (panel i of Figure 4). Upon interaction with the surface, it becomes partially occupied and metallic. Electron states with Fe d_{z^2} character can be found across the Fermi level, with a marked p-DOS increase between −0.5 and 0.5 eV. One of these states, labeled as m_4, is displayed in panel p of Figure 4.

The analysis of the Fe d and Au d p-DOS reported in Figure 5 provides further insight into the molecular hybridization with substrate states. First, we notice that the m_2 state, which mostly involves the in-plane $d_{x^2-y^2}$ and d_{xy} orbitals (panels a, b), is weakly coupled to the Au metal states. The out-of-plane m_1 and m_5 states, involving correspondingly the d_{xz} and d_{yz} (panels c, d), show instead distinct mixing with the metal Au d_{xz} and d_{yz} states (panels h, I green dashed lines). The main FePc/surface interaction is due to the spin-down Fe d_{z^2} (panel e), which is completely hybridized with the spin-down Au d_{z^2} orbital directly underneath the Fe center (panel l, green dashed lines), particularly around the Fermi level.

In addition, this analysis provides evidence of the molecular symmetry change induced by the interaction with the surface. We have shown that the m_2 states present important analogies with the unoccupied spin-down b_{2g} MO. However, in the D_{4h} molecular symmetry of the free FePc molecule, the d_{xy} is the only Fe d orbital that can contribute to the b_{2g} MO. When the FePc interacts with the surface, the m_2 state has both d_{xy} and $d_{x^2-y^2}$ character. These latter Fe d states are energy degenerate. The Fe d_{xz} and d_{yz} states mix into the m_1 and m_5 states, which we associated to the e_g MO. The degeneracy of both the (d_{xy},

dx.doi.org/10.1021/jp300663t | J. Phys. Chem. C 2012, 116, 8657–8663

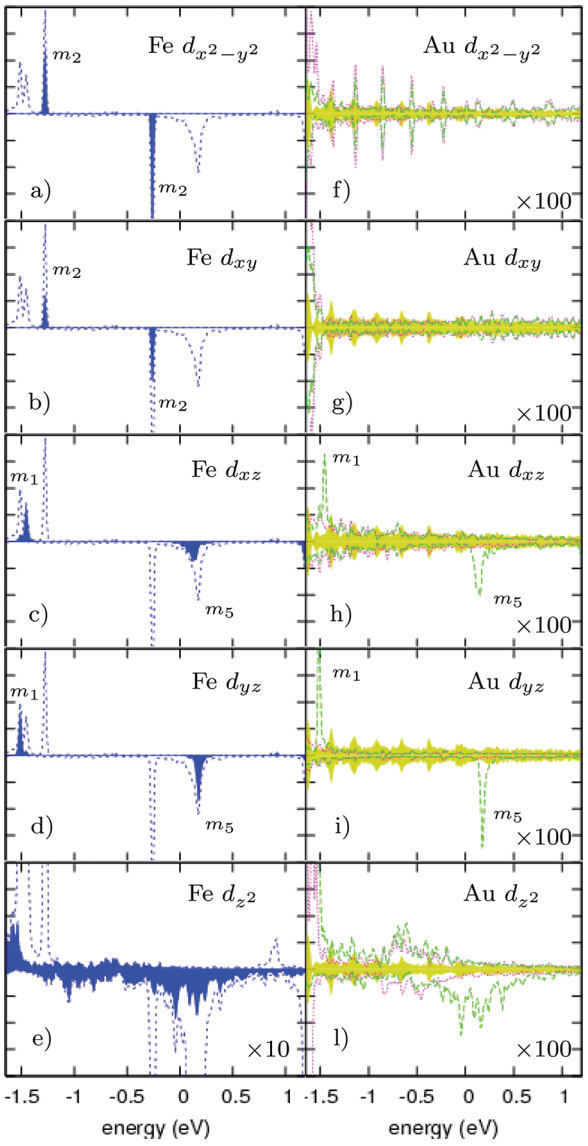

Figure 5. Fe and Au d-components: (a–e) projection on Fe d orbitals, the total Fe d pDOS (blue dashed line) and the pDOS on each orbital (blue filled area); (f–l) projections on Au orbitals, we compare the Au underneath the Fe (green dashed line), with that belonging to the same chain furthest away from the Fe (pink dotted line), and with a bulk Au atom (filled gold area).

$d_{x^2-y^2}$) and (d_{xz}, d_{yz}) orbital pairs point to a molecular symmetry inconsistent with D_{4h}, but compatible with a trigonal bipyramidal geometry of the ligands around the metal center. This is indeed consistent with the structural deformation resulting from the minimum-energy adsorption geometry. The two opposite benzene groups bend upward breaking the D_{4h} symmetry, whereas the Fe ion is pulled away from the molecular plane by 0.16 Å toward the underlying Au atom, thus leading it toward the center of a pyramidal site formed by the four N atoms and the Au surface.

DISCUSSION

The calculated p-DOS can be compared with the photoemission results, taking into account the photoionization cross-section as a function of photon energy.[36] We observed the peak B, resonant with the Au d-bands, decreasing its intensity upon increasing photon energy, thus associated to an electronic state mainly located on the macrocycle. Its mixing with Fe-associated states (see spin-up m_1 and m_2 states in theory Figure 4) and its resonant nature with the underlying Au bands explain its line shape modification as a function of photon energy. Recently, we have determined for this state a tiny energy dispersion along the chains due to the overlapping of molecular levels of the FePc,[22] CoPc[22] and CuPc[37] molecules arranged along Au channels, thus indicating a molecule–molecule interaction independent of the central metallic ion configuration. At higher energies, between −0.6 and −0.5 eV, there are two m_3 states fully localized on the organic macrocycle, corresponding to the a_{1u} orbital of the isolated molecule, in agreement with the experimental observation of the valence band structure H (Figure 1). The low-BE FePc-induced states A and A′ (Figure 2, left panel) can be attributed to hybridized states between the molecular levels localized on the central metal atom and the electronic states of the underlying metal. In particular, the presence of d-symmetry levels associated to the phthalocyanine central Fe atom can be envisaged in both A and A′, due to their photon energy dependence: in fact, their intensity definitely grows upon increasing the photon energy, in good agreement with the relative excitation cross section of C 2p and Fe 3d electronic states.[36] The state A derives from partial occupation of the d_{z^2} level, filled by charge coming from the gold substrate and corresponds to the occupied part of the energy-dispersed m_4 state. A′ is located in the molecular plane, involving $d_{x^2-y^2}$–d_{xy} states, corresponding to the calculated m_2 in-plane state. The unoccupied m_5 states at higher energies involves the Fe d_{yz} and d_{xz} orbitals. Overall, all states with a Fe d_{z^2} character display the strongest mixing with the metal substrate.

Complementary to these state occupation, the first empty states assessed by the photoexcited Fe 2p electrons present an out-of-plane symmetry (peak C of the NEXAFS spectrum and energy-dispersed m_4 state of theory). The absorption edge of structure C and pre-edge of C′ can be attributed to the computed m_5 level. Higher lying states (C′ structure in NEXAFS) are excited with in-plane polarization and correspond to the higher lying 1.2 eV spin–orbit split in-plane b_{1g} ($d_{x^2-y^2}$) states. The interaction of the FePc molecules on the Au(110) substrate induces a strong white-line reduction of d_{z^2}-character (a_{1g}-symmetry) states as observed in a previous experiment,[22] whereas the states located in the molecular plane (peak C′) are almost unaffected by the interaction process. The C′ pre-edge is related to mixed d_{xy}–d_{xz} orbitals with a minor dichroic response. This process of partial state occupation is accompanied by mixing with the underlying gold states, breaking the D_{4h} symmetry of the purely molecular levels. The most notable effect of the molecule/surface interaction is the Fe d_{z^2} molecular orbital mixing with the metal states. This molecular orbital dominates both the states close to Fermi in the supported molecule (panel e of Figure 5), in agreement with the spectroscopic data reported above, showing that the frontier orbitals around the Fermi level have a strong weight on the out-of-plane Fe 3d states. As a result, the Fe d orbitals do not span the same irreducible representation as in the isolated molecule, but are mixed, as observed for other MPcs with a transition metal atom with unfilled d states interacting with a metal substrate.[38−44] At variance with the free-standing FePc case, this agreement shows that the level of theory used in the present work can capture at the semiquantitative level the relative energy and symmetry of the molecular levels when the FePc is supported on the metal surface. Because of the well-known underestimation of the molecular HOMO–LUMO gap

dx.doi.org/10.1021/jp300663t | J. Phys. Chem. C 2012, 116, 8657–8663

by this DFT approach, these energy levels are contracted around the Fermi energy with respect to their experimental counterparts.

CONCLUSIONS

The orbital symmetry of the molecular states of FePc chains arranged along the Au(110) channels has been determined by combining complementary experimental and theoretical methods, bringing to light the broken 4-fold symmetry of the molecular orbitals mainly located on the central metal atom. The symmetry reduction is determined by the complex interplay between electronic effects due to the central metal and the metallic states, and the interaction process induces geometrical effects due to molecular deformation and the underlying substrate rearrangement. The out-of-plane and in-plane d-states associated to the central Fe atom of FePc observed by valence band photoemission and absorption spectroscopy have a one-to-one correspondence with DFT calculations. The results of this combined experimental and theoretical work constitute a solid step toward tailoring of potential magnetic devices, exploiting the nature of these interaction electronic states located on the Fe central atom, close to the Fermi level.

ASSOCIATED CONTENT

Supporting Information

Lowest energy FePc/Au(110) reconstructed interface with ×5 periodicity. This material is available free of charge via the Internet at http://pubs.acs.org.

AUTHOR INFORMATION

Corresponding Author

*E-mail: maria.grazia.betti@roma1.infn.it.

Notes

The authors declare no competing financial interest.

ACKNOWLEDGMENTS

We thank the Elettra national facility of synchrotron radiation and in particular the ALOISA and POLAR beamlines staffs, the Sapienza Università di Roma, and the PRIN project N. 2008525SC7 of MIUR for support. We acknowledge the CINECA Award N. HP10CABDLS, 2011 for the availability of high performance computing resources, and the funding under the "Young SISSA Scientists' Research Projects" scheme 2011-2012, promoted by the International School for Advanced Studies (SISSA), Trieste, Italy.

REFERENCES

(1) Barth, J. V.; Costantini, G.; Kern, K. *Nature* **2005**, *437*, 671−9.
(2) Gambardella, P.; et al. *Nature Mat.* **2009**, *8*, 189−93.
(3) Carbone, C.; et al. *Adv. Funct. Mater.* **2011**, *21*, 1212−1228.
(4) Wende, H.; et al. *Nature Mat.* **2007**, *6*, 516−20.
(5) Tsukahara, N.; Noto, K. I.; Ohara, M.; Shiraki, S.; Takagi, N.; Shin, S.; Kawai, M. *Phys. Rev. Lett.* **2009**, *102*, 1−4.
(6) Brede, J.; Atodiresei, N.; Kuck, S.; Lazić, P.; Caciuc, V.; Morikawa, Y.; Hoffmann, G.; Blügel, S.; Wiesendanger, R. *Phys. Rev. Lett.* **2010**, *105*, 1−4.
(7) Hieringer, W.; Flechtner, K.; Kretschmann, A.; Seufert, K.; Auwärter, W.; Barth, J. V.; Görling, A.; Steinrück, H.-P.; Gottfried, J. M. *J. Am. Chem. Soc.* **2011**, *133*, 6206−22.
(8) Mugarza, A.; Krull, C.; Robles, R.; Stepanow, S.; Ceballos, G.; Gambardella, P. *Nature Commun.* **2011**, *2*, 490.
(9) Cook, P. L.; Liu, X.; Yang, W.; Himpsel, F. J. *J. Chem. Phys.* **2009**, *131*, 194701.
(10) Papageorgiou, N.; Ferro, Y.; Layet, J. M.; Giovanelli, L.; Mayne, a. J.; Dujardin, G.; Oughaddou, H.; Le Lay, G. *Appl. Phys. Lett.* **2003**, *82*, 2518.
(11) Peisert, H.; Liu, X.; Olligs, D.; Petr, A.; Dunsch, L.; Schmidt, T.; Chassé, T.; Knupfer, M. *J. Appl. Phys.* **2004**, *96*, 4009.
(12) Floreano, L.; Cossaro, A.; Gotter, R.; Verdini, A.; Bavdek, G.; Evangelista, F.; Ruocco, A.; Morgante, A.; Cvetko, D. *J. Phys. Chem. C* **2008**, *112*, 10794−10802.
(13) Forrest, S. R. *Nature* **2004**, *428*, 911−8.
(14) Temirov, R.; Soubatch, S.; Luican, A.; Tautz, F. S. *Nature* **2006**, *444*, 350−3.
(15) Ferretti, A.; Baldacchini, C.; Calzolari, A.; Di Felice, R.; Ruini, A.; Molinari, E.; Betti, M. G. *Phys. Rev. Lett.* **2007**, *99*, 046802.
(16) Baldacchini, C.; Mariani, C.; Betti, M. G.; Vobornik, I.; Fujii, J.; Annese, E.; Rossi, G.; Ferretti, A.; Calzolari, A.; Di Felice, R.; Ruini, A.; Molinari, E. *Phys. Rev. B* **2007**, *76*, 245430.
(17) Annese, E.; Fujii, J.; Baldacchini, C.; Zhou, B.; Viol, C.; Vobornik, I.; Betti, M. G.; Rossi, G. *Phys. Rev. B* **2008**, *77*, 1−5.
(18) Chang, S. H.; Kuck, S.; Brede, J.; Lichtenstein, L.; Hoffmann, G.; Wiesendanger, R. *Phys. Rev. B* **2008**, *78*, 233409.
(19) Heinrich, B. W.; Iacovita, C.; Brumme, T.; Choi, D.-J.; Limot, L.; Rastei, M. V.; Hofer, W. a.; Kortus, J.; Bucher, J.-P. *J. Phys. Chem. Lett.* **2010**, *1*, 1517−1523.
(20) Cuadrado, R.; Cerdá, J. I.; Wang, Y.; Xin, G.; Berndt, R.; Tang, H. *J. Chem. Phys.* **2010**, *133*, 154701.
(21) Gargiani, P.; Angelucci, M.; Mariani, C.; Betti, M. G. *Phys. Rev. B* **2010**, *81*, 085412.
(22) Betti, M. G.; Gargiani, P.; Frisenda, R.; Biagi, R.; Cossaro, A.; Verdini, A.; Floreano, L.; Mariani, C. *J. Phys. Chem. C* **2010**, *114*, 21638.
(23) Fortuna, S.; Gargiani, P.; Betti, M. G.; Mariani, C.; Calzolari, A.; Modesti, S.; Fabris, S. *J. Phys. Chem. C* **2012**, *116*, 6251−6258.
(24) Perdew, J. P.; Burke, K.; Ernzerhof, M. *Phys. Rev. Lett.* **1996**, *77*, 3865−3868.
(25) Scandolo, S.; Giannozzi, P.; Cavazzoni, C.; de Gironcoli, S.; Pasquarello, A.; Baroni, S. *Zeitschrift für Kristallographie* **2005**, *220*, 574−579.
(26) Giannozzi, P.; et al. *J. Phys.: Condens. Matt.* **2009**, *21*, 395502.
(27) Aristov, V.; Molodtsova, O.; Maslyuk, V.; Vyalikh, D.; Bredow, T.; Mertig, I.; Preobrajenski, a.B.; Knupfer, M. *Org. Electron.* **2010**, *11*, 1461−1468.
(28) Evangelista, F.; Ruocco, A.; Pasca, D.; Baldacchini, C.; Betti, M. G.; Corradini, V.; Mariani, C. *Surf. Sci.* **2004**, *566−568*, 79−83.
(29) Evangelista, F.; Ruocco, A.; Corradini, V.; Donzello, M.; Mariani, C.; Betti, M. G. *Surf. Sci.* **2003**, *531*, 123−130.
(30) Bartolomé, J.; Bartolomé, F.; Garca, L. M.; Filoti, G.; Gredig, T.; Colesniuc, C. N.; Schuller, I. K.; Cezar, J. C. *Phys. Rev. B* **2010**, *81*, 195405.
(31) Dale, B. W.; Williams, R. J. P.; Johnson, C. E.; Thorp, T. L. *J. Chem. Phys.* **1968**, *49*, 3441.
(32) Coppens, P.; Li, L.; Zhu, N. J. *J. Am. Chem. Soc.* **1983**, *105*, 6173−6174.
(33) Filoti, G.; Kuz'min, M. D.; Bartolomé, J. *Phys. Rev. B* **2006**, *74*, 134420.
(34) Kuz'min, M.; Hayn, R.; Oison, V. *Phys. Rev. B* **2009**, *79*, 024413.
(35) Marom, N.; Kronik, L. *Appl. Phys. A: Mater. Sci. Process.* **2009**, *95*, 165−172.
(36) Yeh, J.; Lindau, I. *Atomic Data and Nuclear Data Tables* **1985**, *32*, 1−155.
(37) Evangelista, F.; Ruocco, A.; Gotter, R.; Cossaro, A.; Floreano, L.; Morgante, A.; Crispoldi, F.; Betti, M. G.; Mariani, C. *J. Chem. Phys.* **2009**, *131*, 174710.
(38) Hu, Z.; Li, B.; Zhao, A.; Yang, J.; Hou, J. G. *J. Phys. Chem. C* **2008**, *112*, 13650−13655.
(39) Petraki, F.; Peisert, H.; Biswas, I.; Chassé, T. *J. Phys. Chem. C* **2010**, *114*, 17638−17643.

(40) Stepanow, S.; Miedema, P.; Mugarza, A.; Ceballos, G.; Moras, P.; Cezar, J.; Carbone, C.; de Groot, F.; Gambardella, P. *Phys. Rev. B* **2011**, *83*, 4−7.
(41) Sun, J.; Gao, L.; He, X.; Cheng, Z.; Deng, Z.; Lin, X.; Hu, H.; Du, S.; Liu, F.; Gao, H.-J. *Phys. Rev. B* **2011**, *83*, 2−5.
(42) Petraki, F.; Peisert, H.; Latteyer, F.; Aygül, U.; Vollmer, A.; Chassé, T. *J. Phys. Chem. C* **2011**, *115*, 21334−21340.
(43) Schmid, M.; Zirzlmeier, J.; Steinruck, H.-P.; Gottfried, J. M. *J. Phys. Chem. C* **2011**, *115*, 17028−17035.
(44) Annese, E.; Fujii, J.; Vobornik, I.; Rossi, G. *J. Phys. Chem. C* **2011**, *115*, 17409.